New Phytologist

A dominant-negative actin mutation alters corolla tube width and pollinator visitation in *Mimulus lewisii*

Baoqing Ding[1], Fengjuan Mou[1,2], Wei Sun[3], Shilin Chen[3], Foen Peng[4], Harvey D. Bradshaw Jr[4] and Yao-Wu Yuan[1,5]

[1]Department of Ecology and Evolutionary Biology, University of Connecticut, Storrs, CT 06269, USA; [2]Faculty of Forestry, Southwest Forestry University, Kunming 650224, China; [3]Institute of Chinese Materia Medica, China Academy of Chinese Medical Sciences, Beijing 100700, China; [4]Department of Biology, University of Washington, Seattle, WA 98195, USA; [5]Institute for Systems Genomics, University of Connecticut, Storrs, CT 06269, USA

Authors for correspondence:
Baoqing Ding
Tel: +1 860 486 4154
Email: ding.baoqing@gmail.com

Yao-Wu Yuan
Tel: +1 860 486 3469
Email: yuan.colreeze@gmail.com

Received: *22 July 2016*
Accepted: *16 September 2016*

New Phytologist (2017) **213:** 1936–1944
doi: 10.1111/nph.14281

Key words: actin, corolla tube, dominant-negative, *Mimulus*, Pollination.

Summary

- A third of all angiosperm species produce flowers with petals fused into a corolla tube. The various elaborations of corolla tube attributes, such as length, width and curvature, have enabled plants to exploit many specialized pollinator groups. These elaborations often differ dramatically among closely related species, contributing to pollinator shift and pollinator-mediated reproductive isolation and speciation. However, very little is known about the genetic and developmental control of these corolla tube attributes.
- Here we report the characterization of a semi-dominant mutant in the monkeyflower species *Mimulus lewisii*, with a substantial decrease in corolla tube width but no change in tube length. This morphological alteration leads to a ~ 70% decrease in bumblebee visitation rate for the homozygous mutant compared to the wild-type.
- Through bulk segregant analysis and transgenic experiment, we show that the mutant phenotype is caused by a dominant-negative mutation in an actin gene. This mutation decreases epidermal cell width but not length, and probably also reduces the number of lateral cell divisions.
- These results suggest a surprising potential role for a 'housekeeping' gene in fine-tuning the development of an ecologically important floral trait.

Introduction

Ever since Darwin successful predicted the existence of the long-tongued hawk moth species *Xanthopan morganii praedicta* based on the exceptionally long and narrow floral tube (i.e. petal nectar spur) of the Madagascar Star Orchid (*Angraecum sesquipedale*) (Darwin, 1862), the evolution of floral tube elaboration in relation to plant–pollinator interactions has attracted considerable research interest. For example, extensive studies on the genus *Aquilegia* (columbines) suggested that the striking variation of nectar spur length within the genus evolved in an adaptive radiation to fit the different tongue lengths of pre-existing pollinator groups (Grant, 1952; Hodges & Arnold, 1994; Whittall & Hodges, 2007); and that cell anisotropy (i.e. unidirectional cell elongation) is the major determinant of spur length across the genus (Puzey *et al.*, 2012). However, the molecular basis of such anisotropic cell elongation remains elusive.

The nectar spurs of Darwin's orchid and columbines are tubular extensions from the bases of individual petals. A much more common floral tube is formed by the fusion of petals: about one-third of all angiosperms produce flowers with their petals fused into a corolla tube, including the vast majority of taxa in the Asterids (APG III, 2009). Corolla tube attributes such as length, width and curvature are evolutionarily labile and often differ dramatically among closely related species, as found in countless examples, including *Mirabilis* (Grant & Grant, 1983), *Petunia* (Stuurman *et al.*, 2004), *Leptosiphon* (Goodwillie *et al.*, 2006), *Iochroma* (Smith *et al.*, 2008), *Ruellia* (Tripp & Manos, 2008), *Nicotiana* (Kaczorowski *et al.*, 2012), *Pedicularis* (Eaton *et al.*, 2012), *Ipomopsis* (Nakazato *et al.*, 2013) and *Saltugilia* (Landis *et al.*, 2016). The rapid evolution of corolla tube elaborations has enabled these plant species to frequently switch pollinators (e.g. from bees to hummingbirds, from hummingbirds to hawkmoths, from one hawkmoth to another with a longer tongue), contributing to pollinator-mediated reproductive isolation and speciation.

The molecular genetic control of corolla tube elaborations is poorly understood. A few quantitative trait locus (QTL) analyses of corolla tube length or/and width, often as part of a larger analysis of pollination syndromes, have been carried out in *Mimulus* (Bradshaw *et al.*, 1998), *Petunia* (Stuurman *et al.*, 2004), *Leptosiphon* (Goodwillie *et al.*, 2006), *Ipomopsis* (Nakazato *et al.*, 2013) and *Penstemon* (Wessinger *et al.*, 2014). A common theme emerging from these studies is that corolla tube length and width variation between natural species are usually controlled by several loci with small to moderate effect. Unfortunately, in none of these systems have the specific genes and mutations underlying

the QTLs been identified. This is not surprising, given that the foremost plant genetic model system, Arabidopsis, happens to not have a corolla tube. Although a large number of genes controlling flower size and organ growth have been identified in Arabidopsis (reviewed in Krizek & Anderson, 2013; Hepworth & Lenhard, 2014), how these genes relate to the specific elaborations of corolla tubes is completely unknown.

Perhaps a more practical approach to investigate the developmental genetics of corolla tube elaboration is to employ a genetic model plant that *has* a corolla tube. The bumblebee-pollinated monkeyflower species *Mimulus lewisii* is such a model; it has proven to be an excellent system for studying the developmental genetics of ecologically important floral traits, especially those that are difficult or infeasible to study using Arabidopsis (Yuan *et al.*, 2013a, 2014, 2016; Sagawa *et al.*, 2016). As the first step of a systematic effort to elucidate the genetic network underlying corolla tube elaborations, we have generated several ethyl methanesulfonate (EMS) mutants of *M. lewisii* with altered corolla tube attributes. In the present study, we report the characterization of a semi-dominant mutant, ML14257, with a much narrower corolla tube compared to the wild-type but with no change in tube length. This phenotype has a significant impact on pollinator visitation, and is caused by a dominant-negative mutation in a 'housekeeping' actin gene.

Materials and Methods

Plant materials and growth conditions

Ethyl methanesulfonate (EMS)mutagenesis was performed using the *Mimulus lewisii* Pursh inbred line LF10, following Owen & Bradshaw (2011). Another inbred line SL9 was used as the mapping line, as described in Yuan *et al.* (2013a). Plants were grown in the University of Connecticut and University of Washington research glasshouses under natural light supplemented with sodium vapor lamps, ensuring a 16-h day length.

Phenotypic characterization

The ML14257 mutant has pleiotropic effects on the width of both floral and vegetative organs, but has no obvious effects on overall plant height, internode elongation or branching pattern. To quantify the floral trait differences between the wild-type (WT) and mutant plants, we measured the widths of the dorsal, lateral and ventral petal lobe, and the corolla aperture (Fig. 1a) with digital calipers; the latter was measured as a proxy for the corolla tube width. We also measured the lengths of the corolla tube (Fig. 1a) and the dorsal petal lobe. In addition, we measured the lengths and widths of the fourth leaf (the largest leaf) of mature plants (after producing the first flower) to quantify the leaf phenotypic differences between the WT and mutant plants.

In order to assess whether the floral trait difference is due to change in cell number, cell size or both, we embedded samples from the dorsal petal lobe or corolla tube in fingernail polish on microscope slides and peeled off the adaxial cell layers with fine-tipped forceps, leaving only the abxial cell layer (i.e. outer epidermis). Samples were examined and photographed using a Zeiss Axioskop microscope connected to a QImaging MicroPublisher 3.3 RTV camera (QImaging, Surrey, BC, Canada). The length and width of five randomly selected, contiguous cells on each slide were measured using ImageJ (Abramoff *et al.*, 2004; Supporting Information Fig. S1).

Pollination experiments in the glasshouse

For pollination experiments, we used six WT (LF10) and six homozygous mutant plants in the 'Far Peak' room in the University of Washington Botany Glasshouse. One-gallon pots were randomly assigned to a 0.5-m grid. Total flower number for each genotype was equalized each day before beginning observations (Day 1: 95 flowers for each genotype; Day 2: 80; Day 3: 76; Day 4: 56) so that the bumblebees (*Bombus impatiens*; Biobest, Belgium) always experienced an equal frequency of each genotype. The commercially available *B. impatiens* is very closely related to *B. vosnesenskii* (Cameron *et al.*, 2007), the main pollinator of *M. lewisii* in the wild (Schemske & Bradshaw, 1999). Both species are generalists (Harder & Barrett, 1993; Alarcon *et al.*, 2008) and they are nearly identical in size. During the 4-d experimental period, bumblebees were not given supplemental feeding (i.e. all nectar and pollen were foraged from the experimental garden). Observers followed each bee and recorded a visit when the bee put its head or more of its body into the corolla opening (Fig. 1e).

Bulk segregant analysis of the mutant by deep sequencing

Bulk segregant analysis followed Yuan *et al.* (2013a). Briefly, an F_2 population was produced by crossing the homozygous ML14257 mutant (in the LF10 genetic background) and the mapping line SL9. DNA samples from 96 F_2 segregants displaying the homozygous mutant phenotype were pooled with equal representation. A small-insert library (~300 bp) was prepared for the pooled sample and ~368 million paired-end, 125-bp reads were generated using an Illumina HiSeq 2500 platform (BioProject: PRJNA326849). Short reads were aligned to the SL9 pseudoscaffolds using CLC Genomics Workbench 7.0 (Qiagen). The *M. lewisii* SL9 pseudoscaffolds were constructed in the previous study (Yuan *et al.*, 2013a) by aligning individual SL9 contigs to the 14 *M. guttatus* chromosomes (https://phytozome.jgi.doe.gov/pz/portal.html), assuming gene collinearity between *M. lewisii* and *M. guttatus*. The resulting raw SNPs were filtered by depth of coverage, tendency of clustering and variant frequency, as described in Yuan *et al.* (2013a). The SL9 pseudoscaffolds were then scanned for regions enriched with homozygous SNPs to determine the candidate gene interval, because the 96 segregants selected for sequencing all should be homozygous for the LF10 phenotype at the causal locus.

Plasmid construction and plant transformation

In order to test the hypothesis that the semi-dominant phenotype of ML14257 is caused by a dominant-negative

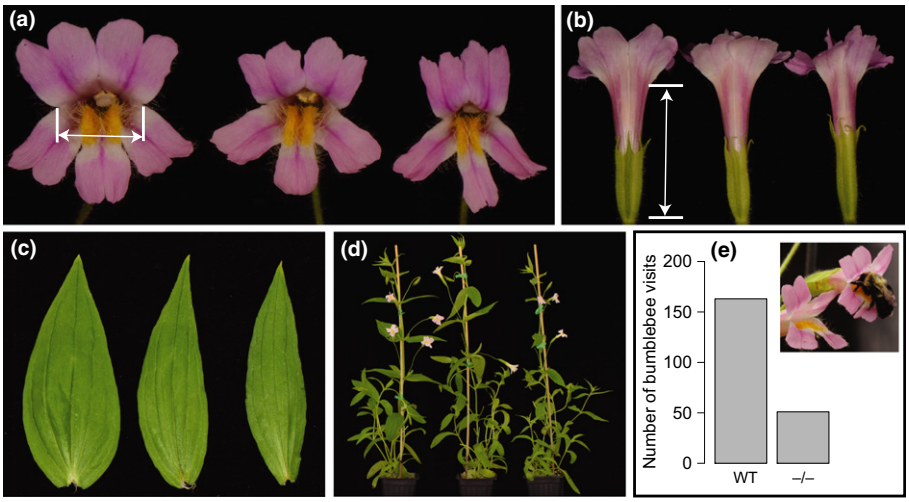

Fig. 1 Effects of a semi-dominant mutation in *Mimulus lewisii* on plant phenotypes and pollinator visitation. (a–d) Images in each sub-panel follow the same order: wild-type (WT) LF10, heterozygous and homozygous mutant (left to right). (a) Front view of the flower. Corolla aperture is marked. (b) Back view of the flower. Corolla tube length is marked. (c, d) The fourth leaf and whole plant at the same developmental stage. (e) Number of total pollinator visits to 307 WT flowers and 307 homozygous mutant (−/−) flowers over a 4-d experimental period. Inset: image of a bumblebee (*Bombus impatiens*) visit on the WT flower.

mutation in the *MlACT1* gene, we constructed a plasmid containing the mutant allele using the pEarleyGate 302 vector (Earley *et al.*, 2006) and transformed it into the WT LF10 background. To generate the plasmid, we first amplified a ~6.3-kb genomic fragment, containing a ~4-kb sequence upstream of the translation initiation codon and the entire *MlACT1* gene (including introns and the 3′ UTR) from the homozygous ML14257 mutant genomic DNA, with Phusion (NEB, Ipswich, MA, USA). The amplified fragment was cloned into the pENTR/D-TOPO vector (Invitrogen) and then a linear fragment containing the *MlACT1* gene flanked by the attL1 and attL2 sites was amplified using M13 primers. This linear fragment subsequently was recombined into the Gateway vector pEarleyGate 302 (Earley *et al.*, 2006). The plasmids were verified by sequencing before being transformed into *Agrobacterum tumefaciens* strain GV3101 for subsequent plant transformation, as described in Yuan *et al.* (2013b). Primers used for plasmid construction and sequencing are listed in Table S1.

Expression analyses by qRT-PCR

RNA extraction and cDNA synthesis followed Yuan *et al.* (2013b). cDNA samples were diluted 10-fold before quantitative reverse transcriptase polymerase chain reaction (qRT-PCR). All qRT-PCR was performed using iQ SYBR Green Supermix (Bio-Rad) in a CFX96 Touch Real-Time PCR Detection System (Bio-Rad). Reactions were run with three biological replicates and a single technical replicate. Samples were amplified for 40 cycles of 95°C for 15 s and 60°C for 30 s. Amplification efficiencies for each primer pair were determined using critical threshold values obtained from a dilution series (1 : 4, 1 : 8, 1 : 16, 1 : 32) of pooled cDNA. *MlUBC* was used as a reference gene as described in Yuan *et al.* (2013b). Relative expression of each target gene compared to the reference gene was calculated using the formula $(E_{ref})^{CP(ref)}/(E_{target})^{CP(target)}$ (Eqn 3 in Pfaffl, 2001). Primers used for qRT-PCR are listed in Table S1.

Results

A semi-dominant mutation in *M. lewisii* affects organ width and pollinator visitation

In order to identify genes that control corolla tube elaborations, we took a forward genetics approach and generated several EMS mutants with altered corolla tube length or/and width. One of them, ML14257, is a semi-dominant mutant with decreased width in both leaf and flower, but with neither a change in organ length, nor any obvious changes in overall plant height, internode elongation or branching pattern (Fig. 1a–d; Table 1). The heterozygous mutant has an intermediate phenotype between the WT and the homozygous mutant (Fig. 1a–d; Table 1). Of particular interest is the corolla tube. In the homozygous mutant, the corolla aperture (i.e. the mouth of the tube; Fig. 1a) is only 8.8 mm in width (Table 1; ~40% decrease compared to the WT) and the tube is < 4.0 mm towards the middle.

Mimulus lewisii is pollinated primarily by the bumblebee species *Bombus vosnesenskii* in its native habitat (Schemske & Bradshaw, 1999). Given the relatively large size of *B. vosnesenskii* workers (abdominal width 5–8 mm; Franklin, 1912), we

Table 1 Measurements of length and width (mm) of petal lobes, corolla tube, and the fourth leaf in *Mimulus lewisii* wild-type (WT) ($n = 39$), heterozygous mutant ($n = 58$) and homozygous mutant ($n = 49$) (mean ± SD)

Trait	WT	Heterozygote	Homozygote
Corolla tube width (aperture)	14.22 ± 0.88	11.59 ± 0.87	8.80 ± 0.64
Dorsal petal width	12.51 ± 0.95	10.24 ± 0.58	8.77 ± 0.61
Lateral petal width	9.58 ± 0.75	8.18 ± 0.58	6.90 ± 0.70
Ventral petal width	9.52 ± 0.70	8.15 ± 0.48	6.67 ± 0.75
Corolla tube length	31.72 ± 1.46	32.54 ± 1.49	30.66 ± 1.35
Dorsal petal length	13.07 ± 0.68	12.79 ± 0.58	12.80 ± 1.06
Leaf width	27.33 ± 4.12	19.6 ± 1.76	13.37 ± 1.12
Leaf length	76.72 ± 10.26	75 ± 5.34	62.63 ± 12.61

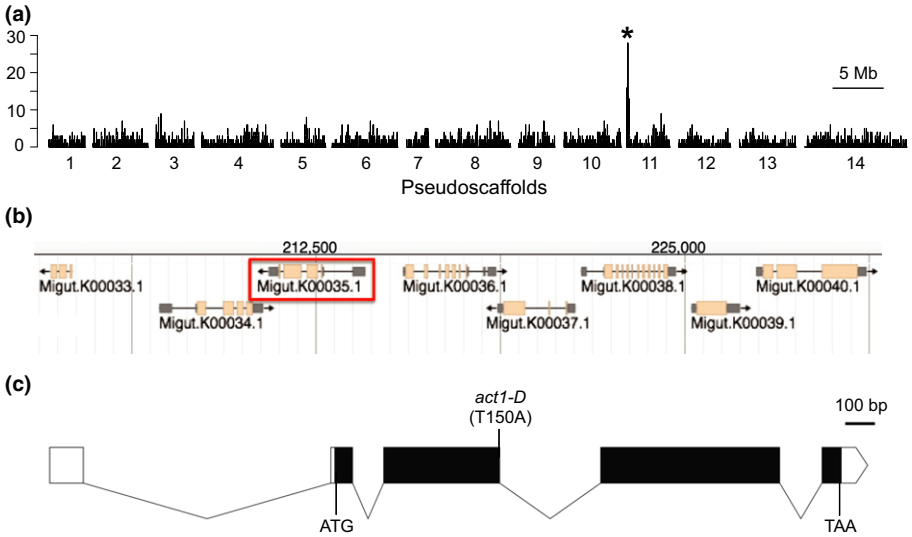

Fig. 2 Bulk segregant analysis of the ML14257 mutant. (a) Genome scan for regions that are enriched in homozygous single nucleotide polymorphisms (SNPs) reveals a sharp peak (indicated by the asterisk). Each pseudoscaffold of the *Mimulus lewisii* SL9 (the mapping line) genome was binned into 20-kb intervals, and the number of homozygous SNPs in each 20-kb interval was plotted in a bar graph. (b) The sharp peak corresponds to a ~30-kb interval in the *Mimulus guttatus* genome (scaffold 11: 203 000–232 000; https://phytozome.jgi.doe.gov/jbrowse/index.html). The *MlACT1* gene is highlighted by a red box. (c) Schematic view of *MlACT1*. A nonsynonymous substitution (A to G) causes the amino acid replacement from Threonine to Alanine at position 150 (T150A). Black box, coding DNA; white box, UTR; line, intron.

predicted that the narrow corolla tube of ML14257 would drastically decrease visitation from *B. vosnesenskii* or related pollinators with a similar size. To test this hypothesis, we performed a pollination experiment in a controlled glasshouse setting. We used *B. impatiens* as the pollinator, as it is nearly identical in size and very closely related to *B. vosnesenskii* (Cameron *et al.*, 2007), and it is commercially available. Our results show a ~70% decrease in bumblebee visitation rate in the homozygous mutant compared to the WT ($\chi^2 = 58.617$, $P < 0.0001$) (Fig. 1e).

A dominant-negative mutation in *MlACT1* underlies the ML14257 mutant phenotype

In order to identify the causal gene underlying the mutant phenotype, we performed a bulk segregant analysis and identified a sharp peak at the beginning of pseudoscaffold 11 (Fig. 2a, indicated by the asterisk), corresponding to a ~30-kb interval in the well-annotated *M. guttatus* genome (https://phytozome.jgi.doe.gov/pz/portal.html) that contains only eight genes (Fig. 2b). It should be noted that, depending on local recombination rate, the size of the candidate interval resulted from a bulk segregant analysis of ~100 *M. lewisii* individuals is not always so small (Y-W. Yuan, unpublished data). Manual inspection of the mutant sequencing reads aligned to the eight genes revealed neither nonsense mutations nor mutations that potentially affect intron splicing. However, one of the genes encoding an actin protein (the *M. lewisii* ortholog of *Migut.K00035*; Fig. 2b) contains a nonsynonymous substitution leading to a threonine-to-alanine replacement (T150A; Fig. 2c). Notably, this threonine residue is perfectly conserved in all actin proteins across plants, animals and fungi (Fig. S2). We reasoned that this T150A replacement is likely to alter protein function and this gene (named *MlACT1* hereafter) is the most promising candidate underlying the mutant phenotype.

Assuming that *MlACT1* is the causal gene (transgenic evidence is described in the next paragraph), two alternative hypotheses can explain the semi-dominance of the mutant phenotype: (1) Haploinsufficiency – the T150A replacement is merely a loss-of-function mutation and a single copy of the WT allele is insufficient for normal *MlACT1* function; (2) Dominant-negative effect – the T150A replacement may interfere with WT actin proteins by disrupting polymerization of actin filaments, as demonstrated by some mis-sense mutations in *Arabidopsis ACT2* and *ACT8* (Nishimura *et al.*, 2003; Kato *et al.*, 2010). A simple experiment to distinguish these two possibilities is to transform the WT plant with the mutant allele. Under the 'haploinsufficiency' scenario, the transgenic lines should not show any abnormal phenotype, unless the transgene causes co-suppression of the endogenous gene, which can be readily tested by qRT-PCR. By contrast, the 'dominant-negative' hypothesis predicts that the transgenic plants will show similar phenotypes to the ML14257 mutant.

We transformed the WT LF10 with a ~6.3-kb genomic fragment amplified from the homozygous ML14257 mutant, including ~4-kb sequence upstream of the ATG initiation codon and the entire *MlACT1* gene (including the 3′ UTR). The transgene differs from the WT allele by a single nucleotide substitution leading to the 'T150A' amino acid replacement. We obtained 12 independent transgenic lines. Six lines show a similar or slightly weaker phenotype than the heterozygous ML14257mutant; three lines are indistinguishable from the homozygous mutant; and unexpectedly, the other three lines show a more severe phenotype than the homozygous mutant, in which even the plant height is drastically reduced (Fig. 3a,b). It should be noted that the same transformation vector, pEarleyGate 302 (Earley *et al.*, 2006),

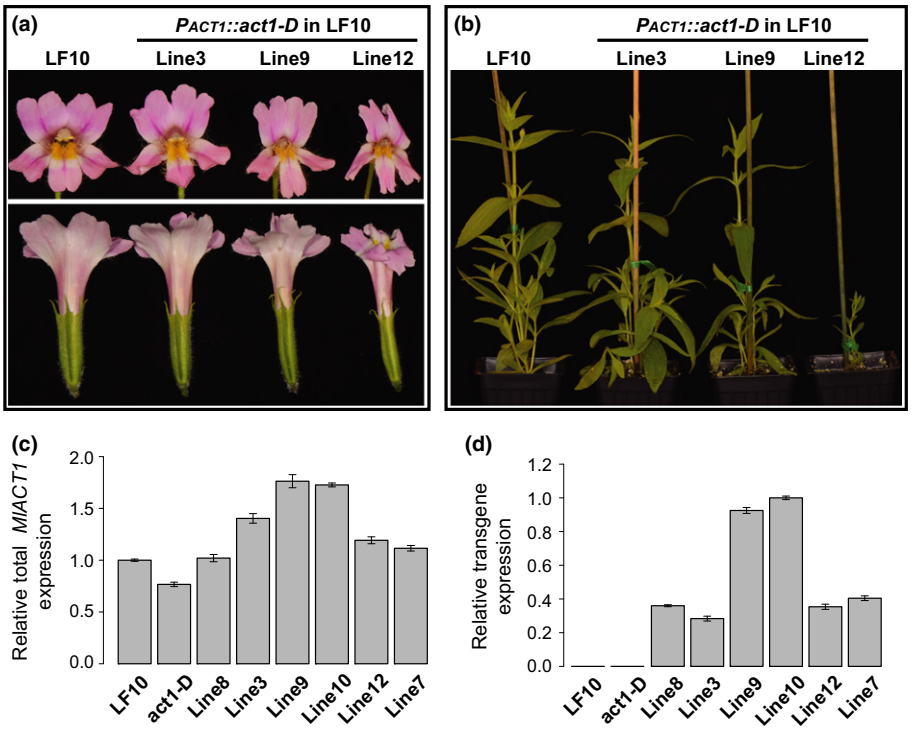

Fig. 3 Transgenic characterization of the dominant-negative allele *act1-D*. (a, b) Transformation of the mutant allele *act1-D* into the wild-type (WT) LF10 background generates transgenic plants with mutant phenotypes. Six lines show phenotypes similar to or slightly weaker than the heterozygous mutant (represented by line 3); three lines are indistinguishable to the homozygous mutant (represented by line 9); and three lines showed a more severe phenotype than the homozygous mutant (represented by line 12). (c) Relative transcript abundance of total *MlACT1* (including the endogenous gene and the transgene), standardized to the WT LF10. Lines 3 and 8 are in the same phenotypic category, so are lines 9 and 10, and lines 7 and 12. (d) Relative transcript abundance of the P_{ACT1}::*act1-D* transgene, standardized to Line 10. *MlUBC* was used as the reference gene for all qRT-PCR experiments. Error bars represent ± 1 SD from three biological replicates.

previously has been used to express pigment-related transgenes in *M. lewisii* (Yuan *et al.*, 2013b, 2016), and none of the > 100 transgenic lines generated in previous studies showed a phenotype resembling the ML14257 mutant. Therefore, the current transgenic results clearly support the 'dominant-negative' hypothesis.

In order to rule out the possibility that the transgenic phenotypes observed are caused by co-suppression, we selected two transgenic lines from each of the three phenotypic categories and compared their *MlACT1* transcript levels with the WT. Although there are seven genes encoding actins in the *M. lewisii* genome (GenBank KX591569–KX591575), they are all quite divergent from one another at the nucleotide level. *MlACT1* and its most similar paralog share only 86% nucleotide identity in the coding sequences (CDS) and, as such, it is straightforward to design gene-specific primers to assay *MlACT1* transcript level. qRT-PCR experiments on 5-mm flower buds using *MlACT1*-specific primers clearly showed that there is no co-suppression in any of the transgenic lines (Fig. 3c). Total transcript level of *MlACT1* in the transgenic lines that phenocopy the homozygous mutant (e.g. lines 9 and 10) is up to 1.7-fold higher than that of the WT, reflecting the expression of the transgenic copy. The difference in *MlACT1* transcript level is less pronounced between the WT and the transgenic lines that show weaker phenotypes (e.g. lines 3 and 8; Fig. 3c). This is consistent with the relatively low expression level of the transgene in these lines compared to lines 9 and 10 (Fig. 3d), as determined by qRT-PCR with one primer from the 3′ end of the *MlACT1* CDS and the other primer from the flanking vector sequence. The gene expression data for the transgenic lines showing the most severe phenotypes (e.g. Lines 7 and 12) are puzzling. The total *MlACT1* transcript levels of these lines are only slightly higher than that of the WT, similar to lines 3 and 8, and the relative transgene expression levels in lines 7 and 12 are also similar to lines 3 and 8 (Fig. 3c,d), yet the phenotype of the former is much stronger than the latter (Fig. 3a,b). What causes the severe phenotype of lines 7 and 12 is unclear at this point.

Taken together, the transgenic experiment and gene expression analysis provide strong evidence that the T150A replacement is a dominant-negative mutation underlying the semi-dominant phenotype (the mutant allele will be referred *act1-D* hereafter). Meanwhile, these results also are direct evidence that *MlACT1* is the causal gene. In this particular case, transformation of the WT allele into the mutant background, a routine procedure to show the causal link between genotype and phenotype, is unlikely to result in full rescue of the phenotype because of the dominant-negative effect.

The *act1-D* allele affects cell width and morphology

In order to understand how the *act1-D* allele reduces organ width (by affecting cell division, cell expansion, or both), we measured the widths of the outer epidermal cells of the dorsal petal lobe and corolla tube for both LF10 and the homozygous *act1-D* mutant. Samples were taken from the same regions of the petal lobe or corolla tube between LF10 and the mutant to ensure proper comparisons. To even out the variation among individual cells within the same sample, all the measurements were done on five contiguous cells (example shown in Fig. S1).

The petal lobe outer epidermal cells of LF10 are jigsaw-puzzle shaped, with interdigitating lobes on the cell margin (Fig. 4a). By contrast, in the homozygous *act1-D* mutant, the outer epidermal cells lack the interdigitating lobes and the cell margins are

characterized by broad wavy lines (Fig. 4a). This observation suggests that the mutant actin protein probably interferes with proper assembly or/and deposition of cortical actin microfilaments in the lobed sites, which is required for localized outgrowth and lobe formation on the margin of leaf pavement cells (Frank & Smith, 2002; Fu *et al.*, 2002, 2005). ANOVA showed significant difference in the width of five contiguous cells between the WT (mean ± SD: 154.7 ± 16.7 μm) and the homozygous mutant (140.7 ± 14.3 μm) ($P < 0.01$), but no difference in cell length (WT: 207.6 ± 28.6 μm; homozygous mutant: 203.3 ± 28.2 μm) ($P > 0.05$) (Fig. 4b). However, the cell width difference (~10% reduction in *act1-D* compared to LF10) is insufficient to explain the total difference in petal lobe width (~30% reduction in *act1-D* compared to LF10; Table 1), which indicates that the *act1-D* mutation probably also reduces lateral cell divisions.

The cell composition of the corolla tube outer epidermis is more complex. In the WT, cells at the top of the tube have prominent protrusions, albeit not as exaggerated as the interdigitating lobes in petal lobe cells; these protrusions become less and less conspicuous towards the base of the corolla tube. We sampled three sections of the corolla tube: immediately below the petal lobe (Top), the middle of the tube (Middle) and the base of the tube (Bottom). In the mutant, even the cells at the top of the tube do not have obvious protrusions (Fig. 4a). The widths of five contiguous cells in the top and middle tube regions of the mutant are reduced by 13% and 11% ($P < 0.05$), respectively, compared to the WT (Fig. 4d). However, cell width at the base of the corolla tube is not significantly different ($P > 0.05$) (Fig. 4d). As in the case of the petal lobe, the cell width reduction in the mutant cannot fully explain the decrease of corolla tube width (~40%), indicating that the number of lateral cell division has also been reduced in the mutant.

Discussion

The evolution of the corolla tube has enabled plants to exploit many specialized pollinator groups (e.g. hawkmoths, long-tongued flies, hummingbirds, nectar bats). Corolla tubes often vary tremendously in length, width and curvature among closely related species, contributing to pollinator shift and pollinator-mediated reproductive isolation and speciation (Stuurman *et al.*, 2004; Nakazato *et al.*, 2013; Wessinger *et al.*, 2014). The *M. lewisii act1-D* mutation causes a narrow tube phenotype and drastically decreases bumblebee visitation rate when tested in a controlled glasshouse setting (Fig. 1e). From an evolutionary point of view, a mutation merely decreasing pollinator visitation in the wild would be inconsequential, as it would lead to lower fitness and be purged from the population rapidly. However, it is tempting to speculate that such narrow-tube mutants may decrease visitation from the original bumblebee pollinator (i.e. *B. vosnesenskii*), while more effectively attracting other pollinators with smaller body sizes (e.g. the smaller sized honeybee *Apis mellifera* accounts for a small proportion of pollinator visits to *M. lewisii* in its native habitat; Schemske & Bradshaw, 1999). Under this scenario, a pollinator shift can be potentially initiated by a single mutation that decreases corolla tube width. It would be of great interest to perform pollination experiments on such mutants not only in the glasshouse, but also in the native habitat of their progenitors.

At first glance it seems surprising that such an ecologically interesting floral phenotype is caused by a coding DNA mutation in a 'housekeeping' gene. Actin is a major cytoskeletal protein that, together with numerous Actin Binding Proteins (ABPs), plays a vital role in plant development and growth (Kandasamy *et al.*, 2007; Blanchoin *et al.*, 2010). However, most plants have multiple actin isovariants with overlapping yet distinct properties; a feature that, on one hand, provides robustness because of functional redundancy and, on the other, allows extraordinary flexibility in cytoskeletal dynamics when different actin monomers with their different ABPs are assembled into actin filaments (Meagher *et al.*, 1999; Li *et al.*, 2015). For example, the *Arabidopsis thaliana* genome contains eight functional actin genes (Meagher *et al.*, 1999). Loss-of-function of single *AtACT* genes produces only mild phenotypes (Gilliland *et al.*, 1998), but ectopic expression of a pollen-specific actin isovariant in nonreproductive organs leads to strong phenotypes, including reduced petal width (Kandasamy *et al.*, 2002), reminiscent of our *M. lewisii act1-D* mutant. In fact, extensive studies in the past two decades have revealed remarkable dynamics of plant actin cytoskeleton (reviewed in Li *et al.*, 2015), in sharp contrast to the conventional perception that cytoskeleton is purely structural and static.

Actin cytoskeleton dynamics are essential for establishing cell polarity and unidirectional cell elongation (e.g. lobe formation on pavement cell margins, pollen tube and root hair growth) (Frank & Smith, 2002; Fu *et al.*, 2002, 2005; Jones *et al.*, 2002; Smith, 2003; Panteris & Galatis, 2005). Interference with the actin cytoskeleton dynamics can lead to loss of interdigitating lobes or protrusions on the cell margin, causing decreased cell width, as observed in the *act1-D* mutant (Fig. 4). Actin cytoskeleton also plays a critical role in regulating cell division. Actin filaments form different arrays in every cell division phase and constantly rearrange from one phase to the next, providing mechanical support, trafficking intracellular vesicles, ensuring correct spindle orientation and pushing the cell cycle forward (reviewed in Liu *et al.*, 2011). The T150A amino acid replacemnt in the *act1-D* mutant locates at an extremely conserved site (Fig. S2) and, therefore, is likely to alter the actin protein structure or/and its interaction with the various ABPs, leading to delay of cell cycle progression and fewer rounds of cell divisions, as indicated by our measurments of floral organ width and cell width.

The most remarkable feature of the *M. lewisii act1-D* mutant is that the mutation only affects lateral expansion without noticeable effect on the longitudinal axis. Although the precise mechanism underlying this unidirectional alteration is yet to be determined, this example highlights the potential significance of cytoskeleton dynamtics in fine-tuning plant organ development and generating ecologically interesting floral tube phenotypes. Another striking example comes from columbines (*Aquilegia*). Perturbation with a microtubule depolymerization agent in *A. chrysantha*, a species with extremely long and slender nectar

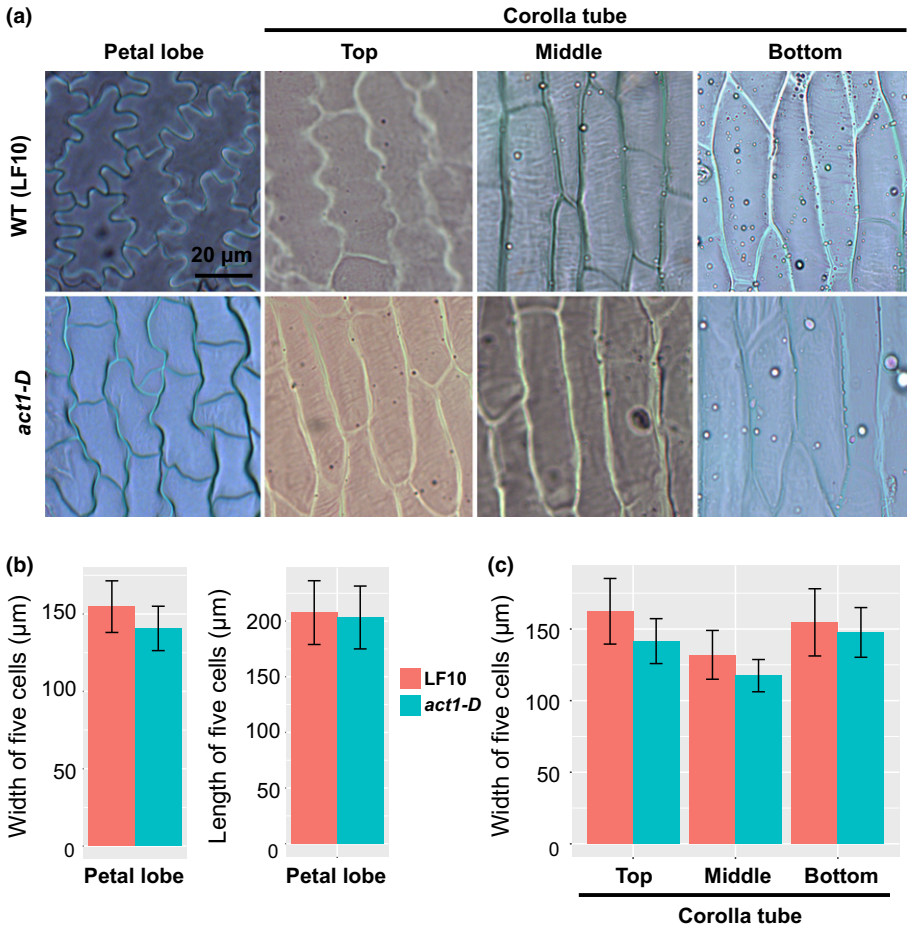

Fig. 4 Effects of the *act1-D* allele on epidermal cell size and morphology in *Mimulus lewisii*. (a) In the wild-type (WT), outer epidermal cells of the petal lobe show jigsaw-puzzle shaped protrusions. The protrusions become less conspicuous when moving from the petal lobe towards the base of the corolla tube. In the *act1-D* mutant, the cell protrusions are much less prominent than in the WT. (b) Petal lobe epidermal cell width is reduced by ~10% in the mutant ($n = 30$) relative to the WT ($n = 30$), but length is not significantly different. (c) In the corolla tube, the width of cells in both top and middle regions are significantly reduced (by 13% and 11%, respectively) in the mutant ($n = 30$) compared to the WT ($n = 30$). But no significant difference was found for the cells at the base of the corolla tube. Error bars represent ± 1 SD.

spur, resulted in a much shorter and wider nectar spur reminiscent of other *Aquilegia* species (Puzey *et al.*, 2012).

An important unresolved issue is whether actin mutations *per se* play a role in generating the incredible diversity of corolla tube structure in nature. An unbiased approach to testing this hypothesis is fine-scale QTL mapping between closely related species that have drastically different floral tube attributes. Given the power of high throughput sequencing these days, researchers are no longer limited by the number of single nucleotide polymorphism markers and fine-scale QTL mapping should be feasible in many plant systems.

Regardless of whether actin mutations turn out to be important in explaining natural variation or not, mutant analysis is valuable, because a deep understanding of the genetic basis of natural variation in any trait requires a comprehensive characterization of the genetic network and developmental or biochemical pathway(s) that control that trait in model systems, which is often achieved through analyzing induced mutants. Perhaps the best example demonstrating this point is anthocyanin pigmentation. More than a dozen structural and regulatory genes controlling anthocyanin pigmentation have been characterized through mutant analysis in model systems such as *Arabidopsis*, maize, petunia and snapdragon (reviewed in Glover, 2014). This network of enzyme-encoding genes and transcription factors is so well understood that one can readily predict, based on differential pleiotropy (Stern, 2000; Carroll, 2005; Streisfeld & Rausher, 2011), that mutations in the R2R3-MYB component of the regulatory complex play a predominant role in generating natural variation in anthocyanin pigmentation (Sobel & Streisfeld, 2013). A systematic effort towards elucidating the genetic network underlying corolla tube elaborations through analysis of corolla tube mutants (e.g. *act1-D* in *M. lewisii*) is required to reach an understanding as deep as that of anthocyanin pigmentation and to predict what are the most important genes and mutations underlying corolla tube variation in nature.

Acknowledgements

We thank Clinton Morse, Matt Opel and Brian Watson for extraordinary plant care in the UConn EEB Research Glasshouses and UW Botany Glasshouses. We thank Brian Watson for assistance in EMS mutagenesis, and Marissa Craig and Lakshmi Panjini for assistance in pollination experiments. We are grateful to Dr Cindi Jones for sharing her microscope and providing technical assistance for cell measurements. This work was supported by the University of Connecticut start-up funds and an NSF grant (IOS-1558083) to Y-W.Y., and in part by an NIH grant (5R01GM088805) to H.D.B.

Author contributions

B.D. and Y-W.Y. planned and designed the research; B.D. performed most of the phenotypic characterization and functional experiments; F.M. contributed to the transgenic experiment; W.S. and S.C. contributed the Illumina sequence data; F.P. and H.D.B. performed pollination experiments; Y-W.Y. performed bulk segregant analysis; and B.D. and Y-W.Y. wrote the manuscript with input from all authors.

References

Abramoff MD, Magalhaes PJ, Ram SJ. 2004. Image processing with ImageJ. *Biophotonics International* **11**: 36–42.

Alarcon R, Waser NM, Ollerton J. 2008. Year-to-year variation in the topology of a plant-pollinator interaction network. *Oikos* **117**: 1796–1807.

Blanchoin L, Boujemaa-Paterski R, Henty JL, Khurana P, Staiger CJ. 2010. Actin dynamics in plant cells: a team effort from multiple proteins orchestrates this very fast-paced game. *Current Opinion in Plant Biology* **13**: 714–723.

Bradshaw HD, Otto KG, Frewen BE, McKay JK, Schemske DW. 1998. Quantitative trait loci affecting differences in floral morphology between two species of monkeyflower (*Mimulus*). *Genetics* **149**: 367–382.

Cameron S, Hines H, Williams P. 2007. A comprehensive phylogeny of the bumble bees (*Bombus*). *Biological Journal of the Linnean Society* **91**: 161–188.

Carroll SB. 2005. Evolution at two levels: on genes and form. *PLoS Biology* **3**: e245.

Darwin C. 1862. *On the various contrivances by which British and foreign orchids are fertilised by insects, and on the good effects of intercrossing*. London, UK: John Murray.

Earley KW, Haag JR, Pontes O, Opper K, Juehne T, Song KM, Pikaard CS. 2006. Gateway-compatible vectors for plant functional genomics and proteomics. *Plant Journal* **45**: 616–629.

Eaton DA, Fenster CB, Hereford J, Huang S-Q, Ree RH. 2012. Floral diversity and community structure in *Pedicularis* (Orobanchaceae). *Ecology* **93**: S182–S194.

Frank MJ, Smith LG. 2002. A small, novel protein highly conserved in plants and animals promotes the polarized growth and division of maize leaf epidermal cells. *Current Biology* **12**: 849–853.

Franklin HJ. 1912. The Bombidae of the new world. *Transactions of the American Entomological Society* **38**: 177–486.

Fu Y, Gu Y, Zheng Z, Wasteneys G, Yang Z. 2005. *Arabidopsis* interdigitating cell growth requires two antagonistic pathways with opposing action on cell morphogenesis. *Cell* **120**: 687–700.

Fu Y, Li H, Yang Z. 2002. The ROP2 GTPase controls the formation of cortical fine F-actin and the early phase of directional cell expansion during *Arabidopsis* organogenesis. *Plant Cell* **14**: 777–794.

Gilliland LU, McKinney EC, Asmussen MA, Meagher RB. 1998. Detection of deleterious genotypes in multigenerational studies. I. Disruptions in individual *Arabidopsis* actin genes. *Genetics* **149**: 717–725.

Glover BJ. 2014. *Understanding flowers and flowering: an integrated approach*. Oxford, UK: Oxford University Press.

Goodwillie C, Ritland C, Ritland K. 2006. The genetic basis of floral traits associated with mating system evolution in *Leptosiphon* (Polemoniaceae): an analysis of quantitative trait loci. *Evolution* **60**: 491–504.

Grant V. 1952. Isolation and hybridization between *Aquilegia formosa* and *A. pubescens*. *Aliso: A Journal of Systematic and Evolutionary Botany* **2**: 341–360.

Grant V, Grant KA. 1983. Hawkmoth pollination of *Mirabilis longiflora* (Nyctaginaceae). *Proceedings of the National Academy of Sciences* **80**: 1298–1299.

Harder LD, Barrett SC. 1993. Pollen removal from tristylous *Pontederia cordata*: effects of anther position and pollinator specialization. *Ecology* **74**: 1059–1072.

Hepworth J, Lenhard M. 2014. Regulation of plant lateral-organ growth by modulating cell number and size. *Current Opinion in Plant Biology* **17**: 36–42.

Hodges SA, Arnold ML. 1994. Columbines: a geographically widespread species flock. *Proceedings of the National Academy of Sciences* **91**: 5129–5132.

Jones MA, Shen J-J, Fu Y, Li H, Yang Z, Grierson CS. 2002. The Arabidopsis Rop2 GTPase is a positive regulator of both root hair initiation and tip growth. *Plant Cell* **14**: 763–776.

Kaczorowski RL, Seliger AR, Gaskett AC, Wigsten SK, Raguso RA. 2012. Corolla shape vs. size in flower choice by a nocturnal hawkmoth pollinator. *Functional Ecology* **26**: 577–587.

Kandasamy MK, Burgos-Rivera BS, McKinney EC, Ruzicka DR, Meagher RB. 2007. Class-specific interaction of profilin and ADF isovariants with actin in the regulation of plant development. *Plant Cell* **19**: 3111–3126.

Kandasamy MK, McKinney EC, Meagher RB. 2002. Functional nonequivalency of actin isovariants in *Arabidopsis*. *Molecular Biology of the Cell* **13**: 251–261.

Kato T, Morita MT, Tasaka M. 2010. Defects in dynamics and functions of actin filament in *Arabidopsis* caused by the dominant-negative actin *fiz1*-induced fragmentation of actin filament. *Plant and Cell Physiology* **51**: 333–338.

Krizek BA, Anderson JT. 2013. Control of flower size. *Journal of Experimental Botany* **64**: 1427–1437.

Landis JB, O'Toole RD, Ventura KL, Gitzendanner MA, Oppenheimer DG, Soltis DE, Soltis PS. 2016. The phenotypic and genetic underpinnings of flower size in Polemoniaceae. *Frontiers in Plant Science* **6**: 1144.

Li J, Blanchoin L, Staiger CJ. 2015. Signaling to actin stochastic dynamics. *Annual Review of Plant Biology* **66**: 415–440.

Liu P, Qi M, Xue X, Ren H. 2011. Dynamics and functions of the actin cytoskeleton during the plant cell cycle. *Chinese Science Bulletin* **56**: 3504–3510.

Meagher RB, McKinney EC, Kandasamy M. 1999. Isovariant dynamics expand and buffer the responses of complex systems: the diverse plant actin gene family. *Plant Cell* **11**: 995–1005.

Nakazato T, Rieseberg LH, Wood TE. 2013. The genetic basis of speciation in the *Giliopsis* lineage of *Ipomopsis* (Polemoniaceae). *Heredity* **111**: 227–237.

Nishimura T, Yokota E, Wada T, Shimmen T, Okada K. 2003. An Arabidopsis *ACT2* dominant-negative mutation, which disturbs F-actin polymerization, reveals its distinctive function in root development. *Plant and Cell Physiology* **44**: 1131–1140.

Owen CR, Bradshaw HD. 2011. Induced mutations affecting pollinator choice in *Mimulus lewisii* (Phrymaceae). *Arthropod-Plant Interactions* **5**: 235–244.

Panteris E, Galatis B. 2005. The morphogenesis of lobed plant cells in the mesophyll and epidermis: organization and distinct roles of cortical microtubules and actin filaments. *New Phytologist* **167**: 721–732.

Pfaffl MW. 2001. A new mathematical model for relative quantification in real-time RT-PCR. *Nucleic Acids Research* **29**: e45.

Puzey JR, Gerbode SJ, Hodges SA, Kramer EM, Mahadevan L. 2012. Evolution of spur-length diversity in *Aquilegia* petals is achieved solely through cell-shape anisotropy. *Proceedings of the Royal Society B* **279**: 1640–1645.

Sagawa JM, Stanley LE, LaFountain AM, Frank HA, Liu C, Yuan YW. 2016. An R2R3-MYB transcription factor regulates carotenoid pigmentation in *Mimulus lewisii* flowers. *New Phytologist* **209**: 1049–1057.

Schemske DW, Bradshaw HD. 1999. Pollinator preference and the evolution of floral traits in monkeyflowers (*Mimulus*). *Proceedings of the National Academy of Sciences, USA* **96**: 11910–11915.

Smith LG. 2003. Cytoskeletal control of plant cell shape: getting the fine points. *Current Opinion in Plant Biology* **6**: 63–73.

Smith SD, Ane C, Baum DA. 2008. The role of pollinator shifts in the floral diversification of *Iochroma* (Solanaceae). *Evolution* **62**: 793–806.

Sobel J, Streisfeld M. 2013. Flower color as a model system for studies of plant evo-devo. *Frontiers in Plant Science* **4**: Article 321.

Stern DL. 2000. Perspective: evolutionary developmental biology and the problem of variation. *Evolution* **54**: 1079–1091.

Streisfeld MA, Rausher MD. 2011. Population genetics, pleiotropy, and the preferential fixation of mutations during adptive evolution. *Evolution* **65**: 629–642.

Stuurman J, Hoballah ME, Broger L, Moore J, Basten C, Kuhlemeier C. 2004. Dissection of floral pollination syndromes in petunia. *Genetics* **168**: 1585–1599.

The Angiosperm Phylogeny Group. 2009. An update of the Angiosperm Phylogeny Group classification for the orders and families of flowering plants: APG III. *Botanical Journal of the Linnean Society* **161**: 105–121.

Tripp EA, Manos PS. 2008. Is floral specialization an evolutionary dead-end? pollination system transitions in *Ruellia* (Acanthaceae). *Evolution* **62**: 1712–1737.

Wessinger CA, Hileman LC, Rausher MD. 2014. Identification of major quantitative trait loci underlying floral pollination syndrome divergence in *Penstemon*. *Proceedings of the Royal Society B* **369**: 20130349.

Whittall JB, Hodges SA. 2007. Pollinator shifts drive increasingly long nectar spurs in columbine flowers. *Nature* **447**: 706–709.

Yuan Y-W, Rebocho AB, Sagawa JM, Stanley LE, Bradshaw HD. 2016. Competition between anthocyanin and flavonol biosynthesis produces spatial pattern variation of floral pigments between *Mimulus* species. *Proceedings of the National Academy of Sciences* **113**: 2448–2453.

Yuan Y-W, Sagawa JM, Di Stilio VnS, Bradshaw HD. 2013a. Bulk segregant analysis of an induced floral mutant identifies a *MIXTA*-like *R2R3 MYB* controlling nectar guide formation in *Mimulus lewisii*. *Genetics* **194**: 523–528.

Yuan Y-W, Sagawa JM, Frost L, Vela JP, Bradshaw HD Jr. 2014. Transcriptional control of floral anthocyanin pigmentation in monkeyflowers (*Mimulus*). *New Phytologist* **204**: 1013–1027.

Yuan Y-W, Sagawa JM, Young RC, Christensen BJ, Bradshaw HD. 2013b. Genetic dissection of a major anthocyanin QTL contributing to pollinator-mediated reproductive isolation between sister species of *Mimulus*. *Genetics* **194**: 255–263.

Supporting Information

Additional Supporting Information may be found online in the Supporting Information tab for this article:

Fig. S1 Illustration of cell length and width measurements.

Fig. S2 Alignment of actin amino acid sequences.

Table S1 Primers used in this study

Please note: Wiley Blackwell are not responsible for the content or functionality of any Supporting Information supplied by the authors. Any queries (other than missing material) should be directed to the *New Phytologist* Central Office.